

**BGD**

12, 1653–1687, 2015

**An ocean  
acidification  
sensitivity study**

A. Weeber et al.

# Seasonality of sea ice controls interannual variability of summertime $\Omega_A$ at the ice shelf in the Eastern Weddell Sea – an ocean acidification sensitivity study

A. Weeber<sup>1</sup>, S. Swart<sup>1,2</sup>, and P. M. S. Monteiro<sup>1,2</sup>

<sup>1</sup>Department of Oceanography, University of Cape Town, Rondebosch 7701, South Africa

<sup>2</sup>Southern Ocean Carbon and Climate Observatory, CSIR – NRE, P.O. Box 320, Stellenbosch, 7599, South Africa

Received: 28 December 2014 – Accepted: 12 January 2015 – Published: 23 January 2015

Correspondence to: A. Weeber (weeber.amy@gmail.com)

Published by Copernicus Publications on behalf of the European Geosciences Union.

Title Page

Abstract

Introduction

Conclusions

References

Tables

Figures



Back

Close

Full Screen / Esc

Printer-friendly Version

Interactive Discussion



## Abstract

Increasing anthropogenic CO<sub>2</sub> is decreasing surface water aragonite saturation state ( $\Omega_A$ ), a growing concern for calcifying Euthecosome pteropods and its wider impact on Antarctic ecosystems. However, our understanding of the seasonal cycle and inter-annual variability of this vulnerable ecosystem remains limited. This study examines surface water  $\Omega_A$  from four consecutive summers in the Eastern Weddell Gyre (EWG) ice shelf region, and investigates the drivers and the role played by the seasonal cycle in the interannual variability of  $\Omega_A$ . Interannual variability in the seasonal phasing and the rate of summer sea ice thaw was found to be the primary factor explaining interannual variability in surface water  $\Omega_A$ . In “optimal” summers when summer sea ice thaw began in late November/early December (2008/2009 and 2010/2011), the summertime increase in  $\Omega_A$  was found to be 1.02, approximately double that from summers when sea ice thaw was delayed to late December (2009/2010 and 2011/2012). We propose that the two critical climate (physical-biogeochemical) sensitivities for  $\Omega_A$  are the timing and the rate of sea ice thaw, which has a direct impact on the mixed layer and the resulting onset and persistence of phytoplankton blooms. The strength of summertime carbonate saturation depends on seasonal changes of sea ice, stratification and primary production. The sensitivity of surface water biogeochemistry in this region to interannual changes in mixed layer – sea ice processes, suggests that future trends in climate and the seasonal cycle of sea ice, combined with rapidly increasing anthropogenic CO<sub>2</sub> will likely be a concern for the Antarctic ice shelf ecosystem within the next few decades. If in the future, primary production is reduced and CO<sub>2</sub> increased, our results suggest that in the EWG summertime surface water aragonite undersaturation will emerge by the middle of this century.

BGD

12, 1653–1687, 2015

### An ocean acidification sensitivity study

A. Weeber et al.

Title Page

Abstract

Introduction

Conclusions

References

Tables

Figures



Back

Close

Full Screen / Esc

Printer-friendly Version

Interactive Discussion



# 1 Introduction

Rising anthropogenic CO<sub>2</sub> is increasing surface water [CO<sub>2</sub>], which decreases ocean pH and alters marine chemistry, a process known as ocean acidification (Doney et al., 2009). Ocean acidification is threatening global marine ecosystems through modifications of fundamental chemical and biological processes (Fabry et al., 2008). Oceans have absorbed approximately a third of the anthropogenic CO<sub>2</sub> added to the atmosphere (Sabine et al., 2004), moderating the effects of climate change (Solomon et al., 2009). This oceanic CO<sub>2</sub> sink is not without consequence – having already caused a 0.1 decrease in surface ocean pH and a shoaling of the calcite and aragonite saturation horizons (Orr et al., 2005). Oceans demonstrate variable sensitivities to changes in pCO<sub>2</sub>, which depend on the buffering capacity of the region (Egleston et al., 2010). High Revelle Factors (Dissolved Inorganic Carbon (DIC) / [CO<sub>3</sub><sup>2-</sup>]) and cold water temperatures are found in Polar Regions, denoting that these areas will be more sensitive to increases in CO<sub>2</sub> (Sabine et al., 2004; Egleston et al., 2010).

As anthropogenic CO<sub>2</sub> levels rise and increase the pCO<sub>2</sub> in surface waters, ocean carbonate ion concentrations [CO<sub>3</sub><sup>2-</sup>] decrease (Caldeira and Wickett, 2003). Marine calcifying organisms such as coccolithophores, pteropods, molluscs and corals rely on carbonate supersaturated (carbonate saturation state ( $\Omega$ ) > 1) waters to minimize energy costs for the formation of their shells and skeletons (Fabry et al., 2008). The effects of naturally, as well as experimentally, elevated seawater pCO<sub>2</sub> on marine calcifiers has been observed to result in a variety of detrimental outcomes, such as decreases in respiration rates (Hennige et al., 2014), reductions in calcification rates (Crook et al., 2013) and reduction growth rates and development (Kroeker et al., 2013). These studies highlight the sensitivity of many calcifying species, and hence ecosystems, to ocean acidification.

Aragonite depositing Euthecosome pteropods are key organisms within the Southern Ocean (SO) ecosystem (Hunt et al., 2008; Bednaršek et al., 2012b). Pteropods, especially the most prominent SO pteropod, *Limacina helicina*, are an important link

## An ocean acidification sensitivity study

A. Weeber et al.

Title Page

Abstract

Introduction

Conclusions

References

Tables

Figures



Back

Close

Full Screen / Esc

Printer-friendly Version

Interactive Discussion



## An ocean acidification sensitivity study

A. Weeber et al.

Title Page

Abstract

Introduction

Conclusions

References

Tables

Figures



Back

Close

Full Screen / Esc

Printer-friendly Version

Interactive Discussion



in the Antarctic trophic structure as both predators and prey, on occasions replacing krill as the principal zooplankton (Cabal et al., 2002; Hunt et al., 2008). Euthecosome pteropods also play a role in the global carbon flux through the sinking of their aragonite shells and faecal pellets (Seibel and Dierssen, 2003). A recent study on SO Euthecosome pteropods showed that in waters where  $0.94 < \Omega_A < 1.12$ , live pteropods experienced shell dissolution, demonstrating the sensitivity of the system to small changes in  $[\text{CO}_3^{2-}]$  (Bednaršek et al., 2012a).

The geographic and weather constrains of the SO limit the availability of in situ data and thus, in the SO, carbonate processes are not very well understood (McNeil and Matear, 2008). Model studies predict mean SO surface waters to become undersaturated with aragonite by the middle of this century (Orr et al., 2005). Taking seasonality into account, McNeil and Matear (2008) propose that south of the Antarctic Polar Front (APF), wintertime aragonite undersaturation may occur as early as 2030, while Mattsdotter Björk., et al. (2014) suggest regional SO summertime surface water  $\Omega < 1$  by the year 2030.

Seasonal phytoplankton blooms assimilate  $\text{CO}_2$  in the euphotic zone, resulting in an increase in  $\Omega_A$  (Orr et al., 2005). The seasonal cycle of phytoplankton blooms in the SO is mediated by PAR, sea ice, water column stability and nutrient supply and how the timing of these processes interact with the phenology of the ecosystem (Thomalla et al., 2011). Thomalla et al. (2011) highlight how the timing of phytoplankton bloom initiation in the marginal ice zone (MIZ) of the SO is critical for extensive and sustained summertime blooms.

Changes in the drivers of mixed layer physics such as sea ice thaw, buoyancy and wind-induced mixing are of key importance to understanding variability in surface water  $\Omega_A$ . Understanding the phasing of the drivers of the seasonal cycle of  $\Omega_A$ , is essential to predict the sensitivity of the carbonate system and the ecosystem to future increases in  $\text{CO}_2$ . In this study we examine the major drivers of the seasonal cycle of  $\Omega_A$  at the Eastern Weddell Gyre (EWG) ice shelf. We investigate how interannual variability in these driving processes drives variability the seasonal cycle of  $\Omega_A$ . Ecosystem impli-

cations of  $\Omega_A$  variability are discussed and future sensitivity of the system to ocean acidification is estimated using very simplified models.

## 2 Methods

Data were collected during the austral summers of 2009–2012 at the EWG ice shelf (68–71° S, 0–10° W) aboard the R/V *SA Agulhas* (Fig. 1).

### 2.1 Underway data

Fugacity of carbon dioxide ( $f\text{CO}_2$ ) was determined quasi-continuously in surface water and in the marine atmosphere with an underway, General Oceanics equilibrator-based system with a Li-COR LI-7000 infra-red gas analyser, designed after Wanninkhof and Thoning (1993) and described by Pierrot et al. (2009). Four reference gases of known  $p\text{CO}_2$  were used: 0.00, 357.32, 377.8 and 427.83 ppm, which were provided and cross-calibrated to international standards by the GAW station at Cape Point. Ancillary instruments logged onto the underway  $p\text{CO}_2$  analyser include a GPS and atmospheric pressure probe situated 5 m above the Licor and equilibrator in a deck housing, intake temperature near the keel at 5 m Depth, a Turner 10-AU fluorometer, a Fluke digital thermometer to measure the equilibrator temperature, a differential barometer to record the equilibrator pressure relative to atmospheric pressure, and an Idronaut multisensor that measures the sea surface temperature (SST) and salinity (SSS). Surface water density ( $\rho$ ) was calculated from SST and SSS using a reference  $\rho$  of  $1027 \text{ kg m}^{-3}$ . The change in density ( $\Delta\rho$ ) from Winter Water (WW), ( $\rho \sim 1027.61 \text{ kg.m}^{-3}$ ) to summer surface water was calculated.

### 2.2 Conductivity-Temperature-Depth (CTD) data

In January 2011 a CTD and Underway CTD (UCTD) transect (64 stations), extending between South Georgia Island and the Antarctic ice shelf (70–58° S, 9–25° W), was

## An ocean acidification sensitivity study

A. Weeber et al.

Title Page

Abstract

Introduction

Conclusions

References

Tables

Figures



Back

Close

Full Screen / Esc

Printer-friendly Version

Interactive Discussion



completed at a nominal spatial resolution of 20 nautical miles. Niskin bottle water samples were collected between the surface to a depth of 300 m in order to measure chl *a*, DIC and Total Alkalinity (TA). In addition a total of 48 CTD profiles were conducted over the austral summers of 2009, 2010, 2011 and 2012 to assess the Antarctic shelf edge physical and biogeochemical processes and related interannual variability (Fig. 5).

To measure DIC and TA, ship based analysis samples were stored in 500 mL bottles with 200  $\mu\text{L}$  of 50 % HgCl (Mercuric Chloride) solution. These samples were analysed in situ using the Marianda Versatile Instrument for the determination of total inorganic carbon and titration alkalinity (VINDTA 3C) and Certified Reference Materials (CRMs) were run before and after each batch and every fifth sample was run as a duplicate to determine the accuracy and the reproducibility of the VINDTA. Once the nutrient data was processed, raw TA and DIC data were post-calibrated using the MATLAB script (VINDTA\_CALCALK) by van Hoven. The precision of the DIC and TA data was  $3.10 \mu\text{mol kg}^{-1}$  and  $2.60 \mu\text{mol kg}^{-1}$ , respectively.

### 2.3 Characterisation of Winter Water

Residual WW was estimated to have been located where potential temperature ( $\theta$ ) was at a minimum in the winter mixed layer (WML), as in Jones et al. (2010) and Geibert et al. (2010). This WML water was found between 55–110 m depth (Fig. 2a). WW  $\Omega_A$  was derived from the mean TA and DIC concentrations in the WML. TA and DIC data was only available at specific bottle depths from a CTD section sampled in January 2011, and thus the closest bottle to the WML for each CTD cast was used to calculate a WW  $\Omega_A \sim 1.3$  (Fig. 2a). A contour of  $\Omega_A$  from the ice shelf to  $61.5^\circ \text{S}$  was plotted using the bottle CTD data (Fig. 2b)

### 2.4 Empirical data

Underway sea surface temperature (SST) and sea surface salinity (SSS) data were used as proxy variables to calculate an empirical TA using the equations of Lee et

**BGD**

12, 1653–1687, 2015

## An ocean acidification sensitivity study

A. Weeber et al.

Title Page

Abstract

Introduction

Conclusions

References

Tables

Figures



Back

Close

Full Screen / Esc

Printer-friendly Version

Interactive Discussion



## An ocean acidification sensitivity study

A. Weeber et al.

Title Page

Abstract

Introduction

Conclusions

References

Tables

Figures



Back

Close

Full Screen / Esc

Printer-friendly Version

Interactive Discussion



al. (2006) for the SO region. To determine the magnitude of local anomalies in the calculated TA, we compared the values to in situ surface CTD measured TA from the VINDTA potentiometric titration. The January 2011 CTD casts were used for this comparison, as these CTDs were the only ones where surface TA was measured. Data points were chosen by matching the underway station times to surface water CTD samples in the EWG, as done in Jones et al. (2010). Empirically calculated TA compared well to the measured surface TA ( $r^2 = 0.66$ ; Fig. 3). In the study region ( $68\text{--}71^\circ\text{S}$ ), the mean TA anomaly was  $-3\ \mu\text{mol kg}^{-1}$ , which suggests that in this region the empirical equations may slightly overestimate TA. The precision of the measured DIC and TA data was  $3.10\ \mu\text{mol kg}^{-1}$  and  $2.60\ \mu\text{mol kg}^{-1}$  respectively, which corresponds to a maximum uncertainty of  $\pm 0.05\ \mu\text{mol kg}^{-1}$  in  $\Omega_A$ . This error contributes approximately 6% of the mean seasonal  $\Delta\Omega_A$  amplitude ( $\Delta\Omega_A \sim 0.77$ ).  $f\text{CO}_2$ , TA, SST and SSS were used to calculate DIC and  $\Omega_A$  using the CO2Sys code (Lewis and Wallace, 1998).

To estimate possible surface water  $\Omega_A$  for the middle and end of this century, the CO2Sys programme was used, with  $f\text{CO}_2$  increased to levels predicted by the IPCC “business as usual” scenario and with TA, SST and SSS unchanged from their present values.

### 2.5 Satellite-derived sea ice concentration and surface wind stress

Daily sea ice concentration (percent area coverage by ice) with a resolution of 25 km was obtained from the National Snow and Ice Data Centre (NSIDC). The data was averaged over the ice shelf study area ( $68\text{--}71^\circ\text{S}$ ,  $0\text{--}10^\circ\text{W}$ ) to obtain mean daily sea ice concentrations. Surface wind stress observations ( $\tau$ ,  $\text{N m}^{-2}$  referenced to 10 m above sea level) were obtained from the Seawinds blended product on a 25 km grid at 6 hourly resolution (Zhang, 2006). The 6 hourly estimates were averaged to daily wind fields using midnight as the daily time step.

### 3 Results and discussion

#### 3.1 The characteristics of $\Omega_A$ variability

The four-year data set obtained from the ice shelf in the EWG (Fig. 1) shows a strong seasonal mode of aragonite carbonate saturation ( $\Omega_A$ ), whose phasing and magnitude have an equally strong interannual variability (Fig. 4a–d).  $\Omega_A$  reaches a minimum ( $\sim 1.3$ ) in winter due to convective mixing, the entrainment of  $\text{CO}_2$ -rich Weddell Sea Deep Water (WSDW) and brine rejection, associated with the formation of Winter Water (WW) (Mosby, 1934; Carmack and Foster, 1975; Carmack and Foster, 1977), and winter light limitation of ocean primary productivity (Arrigo et al., 2008; McNeil and Matear, 2008; Thomalla et al., 2011).

$\Omega_A$  increased throughout the summer months of December, January and February but the magnitude and phasing of the observed seasonal cycle showed a strong interannual variability (Fig. 4a–d). The magnitude of the seasonal cycle ( $\Delta\Omega_A = \text{maximum } \Omega_A - \text{winter water } \Omega_A$ ) was found to be relatively low during the summers of 2010 and 2012, 0.46 and 0.59 respectively, while during the summers of 2009 and 2010/2011,  $\Delta\Omega_A$  doubled to 1.02 (Table 1). The phasing of the seasonal maxima also showed a significant interannual variability of about two weeks with the peak being as early as mid-January in 2009, to late January–early February in 2011 and 2012 and as late as 10 February 2010 (Fig. 4a–d).

There are relatively few data sets characterizing the seasonal variability of the carbonate system at the ice shelf ocean domain around Antarctica (Roden et al., 2013, Shadwick et al., 2013; Mattsdotter Björk et al., 2014). The mean  $\Delta\Omega_A$  in our study was calculated to be 0.77, which is very similar to a study by Roden et al. (2013), where they found  $\Omega_A$  at a coastal site in East Antarctica to vary seasonally from 1.19 in winter to 1.92 in summer. Shadwick et al. (2013) looked at the annual cycle of  $\Omega_A$  in Prydz Bay, East Antarctica, 1993–1995, finding a seasonal increase in  $\Omega_A$  of almost 3. This large summer increase in  $\Omega_A$  is likely due to increased summer biological production and high levels of nutrient availability in the bay (Shadwick et al., 2013).

Title Page

Abstract

Introduction

Conclusions

References

Tables

Figures



Back

Close

Full Screen / Esc

Printer-friendly Version

Interactive Discussion



## An ocean acidification sensitivity study

A. Weeber et al.

Title Page

Abstract

Introduction

Conclusions

References

Tables

Figures



Back

Close

Full Screen / Esc

Printer-friendly Version

Interactive Discussion



Interannual variability in the magnitude of the seasonal cycle of  $\Omega_A$  highlights the importance of regional studies at the ice shelf ocean domain around Antarctica, in order for us to begin to understand the vulnerability of the carbon system and ecosystems in this region to century scale increases in anthropogenic atmospheric  $\text{CO}_2$ . The elevated interest in this interannual dataset is that it offers an opportunity to investigate the interannual variability of drivers of  $\Omega_A$  in the EWG and the role of seasonal and intraseasonal modes in defining the climatic sensitivity of this system.

The magnitude and phasing of the summer increase in  $\Omega_A$  at the ice shelf ocean domain around Antarctica is highly correlated to the response of primary production to summer surface boundary layer dynamics (Roden et al., 2013; Shadwick et al., 2013; Taylor et al., 2013; Mattsdotter Björk et al., 2014). Summer primary production in the EWG is a key element to creating a habitat for calcifiers to grow in a reduced thermodynamic stress due to increased primary production (Fig. 5). Elevated mid-summer  $\Omega_A$  and chl *a* in the SO have been shown to be closely related (Mattsdotter Björk et al., 2014), reflecting a coherence in response to variability in buoyancy (temperature and salinity) and wind stress forcing (Figs. 4, 5, 6). Temperature (Fig. 4i–l) and salinity (Fig. 4e–h) reflect an expected seasonal cycle of decreasing salinity with sea-ice thaw forming a shallow mixed layer, which enhances the associated warming rates and strengthens stratification. What is remarkable in our data set are the contrasting magnitudes of both seasonal and intraseasonal variability in surface water temperature, salinity and  $\Omega_A$  observed during this four year period. We propose that the two key drivers of this interannual variability of the seasonal cycle are: the rate of sea ice thaw, which is the primary driver of surface water density (buoyancy forcing) and stratification through its impact on salinity (Figs. 4e–h, 6a–d), and wind stress (Fig. 6e–h), which regulates the mixing fluxes. Seasonal and intraseasonal modulation of stratification and the mixed layer depth through the entrainment of denser WW reflects variability in the relative magnitudes of buoyancy and mixing (Arrigo et al., 2008).

These physical-biogeochemical characteristics of variability indicate that optimal summer primary production is very sensitive to the balance between buoyancy forc-

---

## An ocean acidification sensitivity study

A. Weeber et al.

---

[Title Page](#)[Abstract](#)[Introduction](#)[Conclusions](#)[References](#)[Tables](#)[Figures](#)[Back](#)[Close](#)[Full Screen / Esc](#)[Printer-friendly Version](#)[Interactive Discussion](#)

ing and mixing, which determine the MLD and the magnitude of stratification. Previous studies have related the thaw of sea ice to both buoyancy forcing as well as to changes in iron (dFe) fluxes, and hence primary production (Smith and Nelson, 1986; Sedwick and DiTullio, 1997; Leventer, 2003; Taylor et al., 2013). On this basis we propose the following conceptual model (Fig. 7), which links the three stratification states, primary production and  $\Omega_A$ .

We use a mixed layer stratification proxy,  $\Delta\rho$ , to connect water column dynamics to biogeochemistry, as other physical data was limited.  $\Delta\rho$  is the change in density between WW ( $\rho \approx 1027.61 \text{ kg m}^{-3}$ ) and the summer surface layer (Fig. 4m–p). In the absence of comparable CTD sections, we found  $\Delta\rho$  to be a useful index of the seasonal evolution of the balance between buoyancy and mixing, as well as to calculate the MLD assuming that freshwater was the only source of buoyancy flux. We found that  $\Delta\rho$  variability in the four year dataset can be put into three categories or states that reflect MLD, mixing dynamics and stratification. These three states of  $\Delta\rho$  are synthesised in the conceptual model (Fig. 7). When  $\Delta\rho$  is approximately 0.4 (i.e. moderately stratified) phytoplankton production and  $\Omega_A$  peak ( $\Omega_A > 1.7$ ), whereas when  $\Delta\rho < 0.4$  (weak buoyancy forcing from delayed or slow sea-ice thaw and/or strong wind stress) or  $\Delta\rho > 0.4$  (strong buoyancy forcing from sea-ice thaw and/or weak wind stress), phytoplankton production and summer  $\Omega_A$  ( $\Omega_A < 1.6$ ) are at varying minimum magnitudes (1.3–1.7), (Figs. 4 and 5).

We propose that contemporary variability in the timing, rate and extent of sea-ice thaw, coupled to the wind stress and seasonal solar radiation drive variability in MLD and in primary production (Fig. 5), are the major drivers of seasonal and intra-seasonal variability in surface water  $\Omega_A$  (Figs. 4, 5, 6). The mechanisms are now examined in greater detail.

### 3.2 Mechanisms controlling seasonal and interannual variability of $\Omega_A$

The seasonal and intraseasonal variability of  $\Omega_A$  is dependent on changes in TA and DIC ( $[\text{CO}_3^{2-}] \approx \text{TA} - \text{DIC}$ ), which are both predominantly modulated by sea ice thaw,

## An ocean acidification sensitivity study

A. Weeber et al.

Title Page

Abstract

Introduction

Conclusions

References

Tables

Figures



Back

Close

Full Screen / Esc

Printer-friendly Version

Interactive Discussion



dilution, mixing, and primary production (Sarmiento and Gruber, 2006). The major processes that alter TA are changes in salinity through the addition or removal of freshwater, the formation or dissolution of  $\text{CaCO}_3$  (Ikaite) and photosynthesis through its uptake of  $\text{NO}_3^-$  (Zeebe and Wolf-Gladrow, 2007; Jones et al., 2010; Roden et al., 2013). DIC concentration is also changed by freshwater fluxes through sea-ice melt, by photosynthetic uptake of  $\text{CO}_2$ , which decreases DIC as well as by air-sea gas exchange (Royal Society, 2005; Jones et al., 2010). Changes in temperature and salinity can, through their impact on the solubility product of  $\text{CaCO}_3$ , also drive some indirect variability in  $\Omega_A$  (Zeebe and Wolf-Gladrow, 2001; Millero et al., 2006).

During the four summer years of data in this study, the seasonal extremes of the temperature and salinity properties of the surface boundary layer temperature ranged from supercooled temperatures of  $-2$  and  $0.5^\circ\text{C}$  and high salinities of  $34.1$ – $34.3$  in WW, to a relatively warmer ( $T \sim 0.5^\circ\text{C}$ ) and fresher ( $S \sim 33.2$ – $33.9$ ) Summer Surface Layer (SSL, Fig. 4). These physical constraints support the view that the maximum contribution that seasonal temperature and salinity changes can make to  $\Delta\Omega_A$  at the EWG ice shelf is about  $\sim 0.15$ , which is about 50 % of what is observed for years in which  $\Delta\Omega_A$  remains low (2009/2010 and 2011/2012, Table 1). WW outcrops with a mean  $p\text{CO}_2$  of  $410$ – $415 \mu\text{atm}$ , which means that outgassing to atmospheric equilibrium could also play a role in the adjustment of seasonal  $\Omega_A$ . Assuming that atmospheric  $p\text{CO}_2$  was  $394 \mu\text{atm}$ , degassing would contribute to a  $\Delta\Omega_A \sim 0.14$ . Thus, collectively all non-biological processes could result in a seasonal  $\Delta\Omega_A \sim 0.3$ , which compares closely to the observed  $\Delta\Omega_A$  in the low  $\Omega_A$  summer periods of 2010 ( $\Delta\Omega_A \sim 0.46$ ) and 2012 ( $\Delta\Omega_A \sim 0.59$ , Table 1). The differences between these years are thought to reflect the impact of the late thaw of sea-ice cover (Fig. 6), which would reduce the impact of degassing on  $\Delta\Omega_A$  during the summers of 2009/2010 and 2011/2012.

The relationship between MLD and primary productivity can be seen in Fig. 5. The surface water conditions in Fig. 4 can be linked to the CTD sections of Fig. 5, providing a detailed picture of the coupling of the physics and biology. During periods when the MLD  $< 45$  m, primary production increased and thus  $\Omega_A$  increased. These results show

## An ocean acidification sensitivity study

A. Weeber et al.

Title Page

Abstract

Introduction

Conclusions

References

Tables

Figures



Back

Close

Full Screen / Esc

Printer-friendly Version

Interactive Discussion



that in seasonal conditions, which are sub-optimal to primary productivity, such as in 2009/2010 and 2011/2012 (Fig. 5), physical drivers of  $\Omega_A$  play a dominant but capped role in seasonal  $\Delta\Omega_A$ . This helps constrain one level of climate sensitivity for summer  $\Omega_A$  directly influenced by changes in the surface boundary layer physical properties and its impact on the carbonate equilibrium system. The coherence of the response of  $\Omega_A$  and primary productivity in years when  $\Delta\Omega_A$  magnitude is high ( $\Delta\Omega_A > 1$ ), suggest that, in agreement with observations elsewhere (Shadwick et al., 2013; Mattsdotter Björk et al., 2014), primary production can, under particular seasonal conditions, become the primary driver of  $\Delta\Omega_A$  (Figs. 4 and 5). Primary production is also influenced by the dynamics of stratification and mixing in the surface boundary layer (Thomalla et al., 2011; Mattsdotter Björk et al., 2014). On this basis, we now explore these processes and how they may modulate intra-seasonal and interannual variability of  $\Delta\Omega_A$ .

### 3.3 Surface boundary layer control of seasonal primary production and $\Delta\Omega_A$

Our data suggests that this sensitive carbonate system is, in some years (2008/2009 and 2010/2011), mainly controlled by the response of primary production to surface boundary layer physics ( $\Delta\Omega_A \sim 1.0$ ) and, as discussed earlier, to a far lesser extent by physical dilution and degassing ( $\Delta\Omega_A \sim 0.3$ ). During all years, the extent of summer blooms seemed to be reliant on the complex interaction between the timing and rate of sea ice thaw, its impact on stratification dynamics, the regulation of the supply of nutrients, including dFe (Geibert et al., 2010; Taylor et al., 2013) and alleviation of light limitation (Thomalla et al., 2011). Melting sea ice is the primary source of buoyancy in the ice shelf region of the SO (Smith and Nelson, 1985). Sea ice thaw increases water column stability near the surface and creates a shallow MLD ( $< 45$  m) relative to the deep WW MLD of 150 m (Figs. 5 and 7). This process relieves light limitation and supports summer blooms typically associated with the Marginal Ice Zone (Smith and Nelson, 1985; Arrigo et al., 2008; Bakker et al., 2008; Swart et al., 2012; Taylor et al., 2013; Mattsdotter Björk et al., 2014). Satellite-based estimates of the timing of phytoplankton bloom initiation in the SO Marginal Ice Zone is 1–15 December (Thomalla et

al., 2011; Supplement), which then constrains the maximum length of the bloom period to a 6 weeks from mid-December to end January when the onset of sea-ice formation begins to limit buoyancy and light and supply (Arrigo et al., 2008). Once summer phytoplankton blooms were initiated, their growth and persistence, and thus the extent of the carbonate super-saturation, was controlled by seasonal surface boundary layer dynamics and nutrient supply (Figs. 4 and 5).

Coherence in the intraseasonal and interannual variability of biomass and  $\Omega_A$  (Figs. 4a–d and 5) indicates that there should be similar contrasting scales of variability in the sea ice thaw rates reflected in the physical variables: temperature, salinity and their impact on stratification reflected in the derived bulk density gradient ( $\Delta\rho$ ) and the depth of the MLD. These are now examined in more detail.

In the four summer periods investigated in this study, we have identified two “optimal” scenarios resulting in higher  $\Omega_A$  (summer maximum  $\Omega_A > 2$ ), (Fig. 4a, c) and two extreme low  $\Omega_A$  scenarios (summer maximum  $\Omega_A < 1.7$ ), (Fig. 4b, d). The optimal summer scenarios both had a  $\Delta\rho \sim 0.4$  during the bloom period (Figs. 4 and 5). The extreme low  $\Omega_A$  seasonal states showed  $\Delta\rho < 0.4$  and  $\Delta\rho > 0.4$ .

The austral summer periods of 2008/2009 and 2010/2011, when sea ice thaw began in late November closely phased with critical seasonal PAR (Thomalla et al., 2011), resulted in elevated summer phytoplankton biomass (Fig. 5b, c) and  $\Omega_A$  (Fig. 4a, c). The corresponding seasonal periods in 2009/2010 and 2011/2012 when sea ice thaw began in late in the summer season mid-late December–early January (Fig. 6b, c) resulted in relatively low chl *a* (Fig. 5a, d, e) and low mean  $\Omega_A$  (Fig. 4b, d). Therefore, we propose that the two primary factors influencing the extent of summertime primary production and hence the summer increase in surface water  $\Omega_A$  are the timing of sea ice thaw and the forcing (buoyancy and mixing) controlling stratification and MLD.

In the latter cases two mixed layer dynamics extremes are evident. In 2009/2010 the sea ice thaw (cover < 80 %) was late, corresponding with the very end of December 2009 and very rapid (loss of  $\sim 2.1$  % cover per day), leading to a sharp decrease in salinity ( $\Delta S \sim 0.8$ ), indicative of a strongly stratified shallow mixed layer (MLD < 10 m).

## BGD

12, 1653–1687, 2015

### An ocean acidification sensitivity study

A. Weeber et al.

Title Page

Abstract

Introduction

Conclusions

References

Tables

Figures



Back

Close

Full Screen / Esc

Printer-friendly Version

Interactive Discussion



This period was also characterized by relatively low wind stress ( $\tau < 0.1 \text{ N m}^{-2}$ ), a consequence of which the stratification is further enhanced by relatively rapid warming ( $\Delta t \sim 1.2^\circ\text{C}$ ), resulting in a high  $\Delta\rho$  of between 0.6 and  $1.2 \text{ kg m}^{-3}$  (Figs. 4, 5, 6).

In terms of the conceptual model (Fig. 7), the late onset of the sea ice thaw delays the summer bloom through light limitation (deep MLD and sea ice cover) as well as the onset of buoyancy forcing required to create a shallow summer MLD from the deeper MLDs typical of winter conditions. However, the late onset of thawing also coincides with a stronger heat flux, which elevates the thaw rate significantly ( $\sim 2.1\%$  per day in January) resulting, under low wind stress ( $\tau < 0.1 \text{ N m}^{-2}$ ), in a very shallow (MLD  $< 10 \text{ m}$ ), fresh ( $S \sim 33.6$ ) mixed layer (Fig. 5). Surface layer salinities in the range of 33.2–33.5 and a freshwater flux of  $5\% \text{ day}^{-1}$  is estimated to correspond to a MLD of  $< 10 \text{ m}$ . Here we suggest that although primary production may have been able to respond to the rapid shallowing of the surface mixed layer, the magnitude of the bloom was constrained by the very limited volume of the MLD (Fig. 5a). We propose that the summer bloom rapidly depleted the dFe reservoir within the MLD and, due to low wind stress during late December 2009 and January 2010, nutrients (primarily Fe) were not replenished and thus further summertime primary production was not sustainable. This resulted in a relatively high mean summer  $f\text{CO}_2$  of  $310.5 \pm 24 \mu\text{atm}$  and a mean summer  $\Omega_A$  of  $1.54 \pm 0.07$ .

The second seasonal extreme low  $\Delta\Omega_A$  scenario was observed during the summer of 2011/2012 (Fig. 4d). Delayed sea-ice thaw ( $> 60\%$  cover in early January 2012) and its associated weak buoyancy forcing linked with elevated wind stress ( $\tau > 0.5 \text{ N m}^{-2}$ ) (Fig. 6d, h), resulted in persistence of deep mixed layers (Fig. 5d) typical of winter and reflected by elevated salinities and low temperatures (Fig. 4h, l). With the exception of a three day period in late January 2012,  $\Delta\rho < 0.4$ , suggesting that the water column stability was not sufficient to facilitate a significant summer bloom. There was however a three day period where  $\Delta\rho \sim 0.4$  which coincided with a rapid increase in chl *a* (Fig. 5e) and thus in  $\Omega_A$  (Fig. 4d). In the SO, where light can be a limiting factor for photosynthesis, a deep (MLD  $> 45 \text{ m}$ ), well mixed water column results in mixing phyto-

## BGD

12, 1653–1687, 2015

### An ocean acidification sensitivity study

A. Weeber et al.

Title Page

Abstract

Introduction

Conclusions

References

Tables

Figures



Back

Close

Full Screen / Esc

Printer-friendly Version

Interactive Discussion



plankton below the 1 % light level creating a light limited seasonal regime (Fig. 7). We suggest that this explains the decreased biomass that resulted in the observed high mean summer surface water  $f\text{CO}_2$  of  $322.9 \pm 38 \mu\text{atm}$  and low mean summer  $\Omega_A$  of  $1.51 \pm 0.13$ .

“Optimal” surface water  $\Omega_A$  (1.8–2.2) scenarios occurred during the summers of 2008/2009 and 2010/2011, although the drivers that caused the elevated surface water  $\Omega_A$  differed between those summer seasons. During 2008/2009, sea ice began to thaw in early December (60 % cover: Fig. 6a), creating a surface mixed layer in which phytoplankton could bloom. The mixed layer was characterised by  $\Delta\rho \sim 0.4$  (Fig. 4m). During the summer months,  $\Delta\rho$  increases to around 0.6, but fluctuates as wind stress increases to around  $0.3 \text{ N m}^{-2}$  (Fig. 6e), mixing up deeper waters and replenishing nutrients through entrainment (Fauchereau et al., 2011). Based on an assumption of a 1 m thick sea-ice layer and a salinity decrease of 0.3 (34.2 to 33.9) it is estimated that the MLD was about 40 m deep and therefore within the euphotic zone, creating an optimal bloom environment with sufficient light and nutrients (Fig. 7).

A similar seasonal evolution of elevated  $\Omega_A$  was observed during the summer of 2010/2011, but strong winds ( $\tau > 0.2 \text{ N m}^{-2}$ ) during late December/early January (Fig. 6g) deepened the MLD ( $S \sim 34.2$ ) and limited light necessary for sustained primary productivity (Fig. 5, c). This resulted in a peak in summer  $\Omega_A$  almost two weeks later than in the summer of 2008/2009 (Fig. 4c). During this summer period where  $\Delta\rho \sim 0.4$  and wind stress was generally low ( $\tau < 0.2 \text{ N m}^{-2}$ ) with periodic periods of stronger winds, primary productivity (Fig. 5b, c) and  $\Omega_A$  (Fig. 4c) were high. This summer period falls predominantly into the ‘optimal’ scenario ( $\Delta\rho \sim 0.4$ ) of our conceptual mixed layer model (Fig. 7). In terms of this model,  $\Delta\rho \sim 0.4$  reflects a stratification which is strong enough to sustain the required light conditions as well as deep enough to hold a reservoir of nutrients. During both these “optimal” summer periods, mean surface water  $f\text{CO}_2 < 262 \mu\text{atm}$  and mean summer  $\Omega_A > 1.9$ , which we have attributed to high summertime primary production. This confirms the link between stratification dynamics and primary production as observed by many previous studies (Smith and

**BGD**

12, 1653–1687, 2015

**An ocean  
acidification  
sensitivity study**

A. Weeber et al.

Title Page

Abstract

Introduction

Conclusions

References

Tables

Figures



Back

Close

Full Screen / Esc

Printer-friendly Version

Interactive Discussion



Nelson, 1985; Arrigo et al., 2008; Bakker et al., 2008; Thomalla et al., 2011; Taylor et al., 2013; Mattsdotter Björk et al., 2014) and thus the link between MLD dynamics and  $\Omega_A$ .

As proposed by our conceptual model (Fig. 7) there seems to be a threshold density anomaly  $\Delta\rho$  of around  $0.4 \text{ kg m}^{-3}$ , when surface water stratification supported an amplified response of primary productivity as reflected by large biomass and  $\Omega_A$  anomalies. Two aspects of these seasonal dynamics are notable: firstly, the sensitivity of the seasonal bloom to the phasing of the onset of sea-ice thaw and light flux control, and secondly, the sensitivity of the bloom to the intraseasonal characteristics of the MLD. As discussed earlier, in these systems sea-ice thaw is the primary buoyancy driver with warming from solar heating as a secondary factor which amplifies the primary fresh-water flux-driven stratification. Under optimal seasonal phasing, melting sea ice injects buoyancy into the residual WW in late November/early December when the seasonal PAR light flux is high enough to trigger photosynthesis (Thomalla et al., 2011).

Variability in  $\Omega_A$  can be further understood by looking at the influences of photosynthesis and dilution on TA and DIC. Surface water  $\Omega_A$  is influenced by fresh water fluxes, mainly through dilution of TA and by primary production, mainly through uptake of DIC (Fig. 8). The vector plot (Fig. 8) shows the contribution made by dilution and primary production to the residual evolution of  $\Omega_A$  during an “optimal” summer (2010/2011) and during a low  $\Omega_A$  summer (2012). During the “optimal” summer, early sea ice thaw and strong surface stratification resulted in increased photosynthesis, and thus in  $\Omega_A$  increasing by approximately 0.8 relative to its winter value (Fig. 8). During January 2012 when summer sea ice thaw was relatively late and the stratified summer period very short, primary production was much lower, resulting in a summer  $\Omega_A$  increase limited to approximately 0.4 (Fig. 8). This highlights the importance of sustained summer phytoplankton blooms in increasing surface water  $\Omega_A$  to create a habitat for pteropods where  $\Omega_A$  increases from its winter minimum.

The implications for these contrasting interannual seasonal states for the sensitivity of the system to increasing anthropogenic  $\text{CO}_2$  are now examined.

## BGD

12, 1653–1687, 2015

### An ocean acidification sensitivity study

A. Weeber et al.

Title Page

Abstract

Introduction

Conclusions

References

Tables

Figures



Back

Close

Full Screen / Esc

Printer-friendly Version

Interactive Discussion



### 3.4 Century-scale anthropogenic CO<sub>2</sub> increase and the onset of seasonal carbonate ( $\Omega_A$ ) undersaturation

Atmospheric CO<sub>2</sub> levels are predicted to reach approximately 550  $\mu\text{atm}$  by the middle of the 21st century, and to be double the current value by the end of this century (Steinacher et al., 2009). Studies suggest that oceans, particularly the SO, will continue to take up a decreasing portion of this anthropogenic CO<sub>2</sub> (Sabine et al., 2004; Le Queré et al., 2007; Raupach et al., 2014), increasing the concentration of DIC in the surface waters and resulting in higher sensitivity by  $p\text{CO}_2$  to local variability of DIC and TA (Egleston et al., 2010). Taking the effects of seasonality into account, surface water aragonite undersaturation south of the Antarctic Polar Front is predicted to occur as early as the year 2030 with atmospheric  $p\text{CO}_2$  at about 450  $\mu\text{atm}$  (McNeil and Matear, 2008).

During the winter period in the SO, surface water  $\Omega_A$  reaches a minimum (McNeil and Matear, 2008; Roden et al., 2013; Shadwick et al., 2013; Mattsdotter Björk et al., 2014). McNeil and Matear (2008) examined the role of the seasonal cycle in bringing forward the predicted year of  $\Omega_A$  undersaturation. They show that much of the SO is likely to experience winter  $\Omega_A$  undersaturation by the year 2030, due to the effects of upwelling of DIC rich deep waters and winter mixing. Mattsdotter Björk et al. (2014) analysed surface water carbon characteristics in the Amundsen and Ross Seas during four Austral summers from 2006–2010. They increased SST, SSS and TA by 10  $\mu\text{mol kg}^{-1} \text{decade}^{-1}$  and increased DIC by 5  $\mu\text{mol kg}^{-1} \text{decade}^{-1}$ . Similarly, their results suggest that in the Amundsen and Ross Seas, regional summertime surface water  $\Omega_A$  undersaturation will occur by the years 2026–2030. It is unexpected that both studies, using different techniques and focusing on different regions and different seasons, came up with similar years for  $\Omega_A$  undersaturation in the SO. McNeil and Matear (2008) point out that they do not have data for the ice shelf region and thus that their results may overestimate  $\Omega_A$  close to the ice shelf. These studies highlight the

**BGD**

12, 1653–1687, 2015

## An ocean acidification sensitivity study

A. Weeber et al.

Title Page

Abstract

Introduction

Conclusions

References

Tables

Figures



Back

Close

Full Screen / Esc

Printer-friendly Version

Interactive Discussion



need for increasing the intensity and regional focus of long term observations in the Southern Ocean and Antarctic ice shelf.

Our conceptual model estimated future mean summertime surface water  $\Omega_A$  for an “optimal” summer scenario (data from 2010/2011) and for a low  $\Omega_A$  summer scenario (data from 2011/2012, Table 2). Our estimates suggest that during both the “optimal” and the late ice thaw summer scenarios, surface waters at the EWG ice shelf are not likely to experience summertime  $\Omega_A$  undersaturation before the year 2050, in agreement with Orr et al. (2005). During years when the timing of sea ice thaw is “optimal”, we predict that mean summer surface water  $\Omega_A \sim 1.25 \pm 0.1$  by the year 2050 and  $1.04 \pm 0.13$  by the year 2100 (Table 2), depending on the accuracy of future anthropogenic  $\text{CO}_2$  trajectories. This suggests that if there are sufficient “optimal” summers, the EWG ice shelf region could remain interannually supersaturated with respect to aragonite until the end of this century. Alternatively, during summers when sea ice thaw is out of phase with ecosystem phenology, (either before November or late December/January), surface water  $\Omega_A \sim 1.07 \pm 0.05$  by the year 2050 and  $0.82 \pm 0.07$  by the year 2100 (Table 2). Thus if in the coming century there are an increasing number of summers during which the timing of sea ice thaw is not ‘optimal’, surface water  $\Omega_A \sim 1$  by the middle of this century.

This seasonal variability in summertime  $\Omega_A$  is of concern, as studies propose that with a changing climate both the onset of sea ice formation and thaw will change (Boe et al., 2009) as well as the extent of marine primary production (Steinacher et al., 2010; Yamamoto et al., 2012). Photosynthesis as well as surface water TA are predicted to decrease due to increased stratification (Steinacher et al., 2010; Yamamoto et al., 2012), and this will likely bring forward the year of undersaturation due to the influence of primary production on surface water  $\Omega_A$ .

Our results indicate that the interannual variability of  $\Omega_A$  linked to changes in sea-ice thaw seasonality are an additional consideration when predicting the onset of undersaturation in the EWG ice shelf ecosystem.

## BGD

12, 1653–1687, 2015

### An ocean acidification sensitivity study

A. Weeber et al.

Title Page

Abstract

Introduction

Conclusions

References

Tables

Figures



Back

Close

Full Screen / Esc

Printer-friendly Version

Interactive Discussion



## 4 Ecosystem implications

Studies show that although the majority of calcifying organisms show negative effects in an increased  $\text{CO}_2$  environment, some calcifying organisms demonstrated increased growth rates, highlighting our lack of understanding of these complex processes (Ries et al., 2009). We are mindful of the limitations of  $\Omega_A$  as a predictor of both organism and ecosystem responses to ocean acidification, both because of the non-thermodynamic nature of biological calcification as well as the uncertain boundaries of short term physiological responses and long term adaptation (Ries et al., 2009).

The context of its use here is more as an indicator of increasing physiological stress reflecting the relationship between the trend towards thermodynamic undersaturation and the increasing energetic costs of calcification to an organism such as the Pteropod (Fabry, 2008; Maas et al., 2012). The importance of pteropods to the SO ecosystem as well as to the global oceanic carbon cycle is well known (Comeau et al., 2010; Bednaršek et al., 2012b) and their possible migration or decline is therefore of great concern. A growing trend of stronger than expected interannual variability in the seasonal cycle of  $\Omega_A$  is of concern for the survival of Euthecosome pteropods, a key part of the food web in this region (Hunt et al., 2008; Bednaršek et al., 2012b). Winter minimum values of  $\Omega_A < 1.12$  in the SO have already been shown to affect pteropods ability to maintain their protective shells (Bednaršek et al., 2012a). Pteropods live for 2–3 years so consecutive years of surface water  $\Omega_A \sim 1$ , could have long lasting impacts on the adult pteropod population, the food web and ecosystem.

At no time in the course of this four year data set was the system undersaturated with respect to  $\text{CaCO}_3$  ( $\Omega_A > 1$ ). However, the combined effects of the physiological and energy impacts of low  $\Omega_A \sim 1.5$  and a low energy supply from phytoplankton biomass could point to a recruitment failure in future years with sea ice conditions as observed during 2010 and 2012, in which the balance between ice thaw driven buoyancy forcing and wind mixing are not optimal to support summer primary production. Thus these data suggest that inter and intra seasonal variability in the physics and biogeochemistry

BGD

12, 1653–1687, 2015

### An ocean acidification sensitivity study

A. Weeber et al.

Title Page

Abstract

Introduction

Conclusions

References

Tables

Figures



Back

Close

Full Screen / Esc

Printer-friendly Version

Interactive Discussion



of the surface boundary layer may not only be key factors in ecosystem forcing but may also reflect an additional sensitivity to long term CO<sub>2</sub> forcing of these high latitude systems.

## 5 Conclusions

5 Aragonite saturation state ( $\Omega_A$ ) at the EWG ice shelf showed a strong seasonal cycle, with  $\Omega_A$  reaching a maximum during the summer months of January and February in all years. However there was also significant interannual variability in the magnitude and phasing of the  $\Omega_A$  seasonal cycle. We show that the interannual variability in physical (mixing and buoyancy) processes explained the magnitude and phasing of the summertime phytoplankton bloom and thus  $\Omega_A$ . We propose that summer sea ice  
10 thaw (buoyancy flux) during the first two weeks of December, in phase with ecosystem phenology, resulted in optimal light and nutrient supply in the surface layer that increased primary production and  $\Omega_A > 2$ . In years when sea ice thaw was out of phase with phytoplankton phenology, either too early or too late, summertime surface water  
15  $\Omega_A < 1.7$ , only 0.4 above the winter minimum. We propose that the two critical climate (physical-biogeochemical) sensitivities for  $\Omega_A$  are the timing and rate of sea ice thaw and the resulting onset and persistence of phytoplankton blooms.

As anthropogenic CO<sub>2</sub> increases and sea ice dynamics change with a changing climate, understanding the trend in these characteristics of variability in the seasonal  
20 drivers of  $\Omega_A$  in regions such as the EWG will become increasingly important. Ocean acidification cannot be separated from how the underlying dynamics are changing. Model studies predominantly investigate trends in marine carbonate chemistry over large ocean areas but this study highlights the importance of regional ocean acidification investigations. Localised sub-regional variations in the timing of seasonal sea ice  
25 thaw and in the magnitude of summer primary production make a significant contribution towards a better understanding of the sensitivity and magnitude of impacts on marine biogeochemistry and thus on polar marine ecosystems.

### An ocean acidification sensitivity study

A. Weeber et al.

Title Page

Abstract

Introduction

Conclusions

References

Tables

Figures



Back

Close

Full Screen / Esc

Printer-friendly Version

Interactive Discussion



*Acknowledgements.* This work was supported by the CSIR, the Southern Ocean Carbon – Climate Observatory (SOCCO) Programme and the University of Cape Town. It is a contribution to the CarboChange EU FP7 Project (Grant: 264879). A. Weeber was supported through the NRF and Ma-Re/UCT. S. Swart and P. M. S. Monteiro were supported by CSIR’s PG funding (0000005278), NRF-SANAP grants (SNA2011112600001 and SNA2011120800004) and a CSIR YREF grant (05441) for S. Swart. This work would not have been possible without the dedicated work of the scientists, officers and crew of the SANAE research voyages aboard the R/V *SA Agulhas* and logistical support of DEA-SANAP. We would like to thank H. Waldron for his support during the studentship research work.

## References

- Arrigo, K. R., Van Dijken, G. L., and Bushinsky, S.: Primary production in the Southern Ocean, 1997–2006, *J. Geophys. Res.*, 113, C08004, doi:10.1029/2007JC004551, 2008.
- Bakker, D. C. E., Hoppema, M., Schröder, M., Geibert, W., and de Baar, H. J. W.: A rapid transition from ice covered CO<sub>2</sub>-rich waters to a biologically mediated CO<sub>2</sub> sink in the eastern Weddell Gyre, *Biogeosciences*, 5, 1373–1386, doi:10.5194/bg-5-1373-2008, 2008.
- Bednaršek, N., Tarling, G. A., Bakker, D. C. E., Fielding, S., Jones, E. M., Venables, H. J., Ward, P., Kuzirian, A., Lézé, B., and Murphy E. J.: Extensive dissolution of live pteropods in the Southern Ocean, *Nat. Geosci.*, 5, 881–885, 2012a.
- Bednaršek, N., Tarling, G. A., Fielding, S., and Bakker, D. C. E.: Population dynamics and biogeochemical significance of *Limacina helicina antarctica* in the Scotia Sea (Southern Ocean), *Deep-Sea Res. Pt. II*, 59, 105–116, 2012b.
- Boe, J. L., Hall, A., and Qu, X.: September sea-ice cover in the Arctic Ocean projected to vanish by 2100, *Nat. Geosci.*, 2, 341–343, 2009.
- Caldeira, K. and Wickett, M. E.: Anthropogenic carbon and ocean pH, *Nature*, 425, 365–365, 2003.
- Cabal, J. A., Alvarez-Marqués, F., Acuña, J. L., Quevedo, M., Gonzalez-Quirós, R., Huskin, I., Fernández, D., Rodriguez del Valle, C., and Anadón, R.: Mesozooplankton distribution and grazing during the productive season in the Northwest Antarctic Peninsula (FRUELA cruises), *Deep-Sea Res. Pt. II*, 49, 869–882, 2002.

## An ocean acidification sensitivity study

A. Weeber et al.

Title Page

Abstract

Introduction

Conclusions

References

Tables

Figures



Back

Close

Full Screen / Esc

Printer-friendly Version

Interactive Discussion



## An ocean acidification sensitivity study

A. Weeber et al.

Title Page

Abstract

Introduction

Conclusions

References

Tables

Figures



Back

Close

Full Screen / Esc

Printer-friendly Version

Interactive Discussion



- Carmack, E. C. and Foster, T. D.: On the flow of water out of the Weddell Sea, *Deep-Sea Res.*, 22, 711–724, 1975.
- Carmack, E. C. and Foster, T. D.: Water masses and circulation in the Weddell Sea, in: *Polar Oceans, Proceedings of the Polar Oceans Conference, Montreal, 1974*, edited by: Dunbar, M. J., Arctic Institute of North America, Calgary, Canada, 151–165, 1977.
- 5 Comeau, S., Jeffree, R., Teyssié, J. L., and Gattuso, J. P.: Response of the Arctic Pteropod *Limacina helicina* to Projected Future Environmental Conditions, *PLoS ONE*, 5, e11362, doi:10.1371/journal.pone.0011362, 2010.
- Crook, E. D., Cohen, A. L., Rebolledo-Vieyra, M., Hernandez, L., and Paytan, A.: Reduced calcification and lack of acclimatization by coral colonies growing in areas of persistent natural acidification, *P. Natl. Acad. Sci. USA*, 110, 11044–11049, 2013.
- 10 Doney, S. C., Fabry, V. J., Feely, R. A., and Kleypas, J.: Ocean Acidification: The Other CO<sub>2</sub> Problem, *Annu. Rev. Mar. Sci.*, 1, 169–192, 2009.
- Egleston, E. S., Sabine, C. L., and Morel, F. M.: Revelle revisited: Buffer factors that quantify the response of ocean chemistry to changes in DIC and alkalinity, *Global Biogeochem. Cy.*, 24, GB1002, doi:10.1029/2008GB003407, 2010.
- 15 Fabry, V. J., Seibel, B. A., Feely, R. A., and Orr, J. C.: Impacts of ocean acidification on marine fauna and ecosystem processes, *ICES J. Mar. Sci.*, 65, 414–432, 2008.
- Fauchereau, N., Tagliabue, A., Monteiro, P., and Bopp, L.: The response of phytoplankton biomass to transient mixing events in the Southern Ocean, *Geophys. Res. Lett.*, 38, L17601, doi:10.1029/2011GL048498, 2011.
- 20 Geibert, W., Assmy, P., Bakker, D. C. E., Hanfland, C., Hoppema, M., Pichevin, L. E., Schröder, M., Schwarz, J. N., Stimac, I., Usbeck, R., and Webb, A.: High productivity in an ice melting hot spot at the eastern boundary of the Weddell Gyre, *Global Biogeochem. Cy.*, 24, GB3007, doi:10.1029/2009GB003657, 2010.
- Hennige, S. J., Wicks, L. C., Kamenos, N. A., Bakker, D. C. E., Findlay, H. S., Dumousseaud, C., and Roberts, J. M.: Short-term metabolic and growth responses of the cold-water coral *Lophelia pertusa* to ocean acidification, *Deep-Sea Res. Pt. II*, 99, 27–35, 2014.
- Hunt, B. P. V., Pakhomov, E. A., Hosie, G. W., Siegel, V., Ward, P., and Bernard, K.: Pteropods in Southern Ocean ecosystems, *Prog. Oceanogr.*, 78, 193–221, 2008.
- 30 Jones, E. M., Bakker, D. C. E., Venables, H. J., Whitehouse, M. J., Korb, R. E., and Watson, A. J.: Rapid changes in surface water carbonate chemistry during Antarctic sea ice melt, *Tellus*, 62, 621–635, 2010.

---

**An ocean  
acidification  
sensitivity study**A. Weeber et al.

---

[Title Page](#)[Abstract](#)[Introduction](#)[Conclusions](#)[References](#)[Tables](#)[Figures](#)[Back](#)[Close](#)[Full Screen / Esc](#)[Printer-friendly Version](#)[Interactive Discussion](#)

Kroeker, K. J., Kordas, R. L., Crim, R., Hendriks, I. E., Ramajo, L., Singh, G. S., Duarte, C. M., and Gattuso, J.: Impacts of ocean acidification on marine organisms: quantifying sensitivities and interaction with warming, *Glob. Change Biol.*, 19, 1884–1896, 2013.

Le Quéré, C., Rödenbeck, C., Buitenhuis, E. T., Conway, T. J., Langenfelds, R., Gomez, A., Labuschhagne, C., Ramonet, M., Nakazawa, T., Metzl, N., Gillett, N., and Heimann, M.: Saturation of the Southern Ocean CO<sub>2</sub> Sink Due to Recent Climate Change, *Science*, 316, 1735–1738, 2007.

Lee, K., Tong, L. T., Millero, F. J., Sabine, C. L., Dickson, A. G., Goyet, C., Park, G. H., Wanninkhof, R., Feely, R. A., and Key, R. M.: Global relationships of total alkalinity with salinity and temperature in surface waters of the world's oceans, *Geophys. Res. Lett.*, 33, L19605, doi:10.1029/2006GL027207, 2006.

Leventer, A.: Particulate flux from sea ice in polar waters, in: *Sea ice. An introduction to its physics, chemistry, biology and geology*, edited by: Thomas, D. N. and Dieckmann, G. S., John Wiley & Sons, 303–332, 2003.

Lewis, E. and Wallace, D. W. R.: CO<sub>2</sub>SYN-Program developed for the CO<sub>2</sub> system calculations, Carbon Dioxide Information and Analysis Centre, Report ORNL/CDIAC-105, 1998.

Maas, A. E., Wishner, K. F., and Seibel, B. A.: The metabolic response of pteropods to acidification reflects natural CO<sub>2</sub>-exposure in oxygen minimum zones, *Biogeosciences*, 9, 747–757, doi:10.5194/bg-9-747-2012, 2012.

Mattsdotter Björk, M., Fransson, A., Torstensson, A., and Chierici, M.: Ocean acidification state in western Antarctic surface waters: controls and interannual variability, *Biogeosciences*, 11, 57–73, doi:10.5194/bg-11-57-2014, 2014.

McNeil, B. I. and Matear, R. J.: Southern Ocean acidification: A tipping point at 450-ppm atmospheric CO<sub>2</sub>, *P. Natl. Acad. Sci.*, 105, 18860–18864, 2008.

Millero, F. J., Graham, T. B., Huang, F., Bustos-Serrano, H., and Pierrot, D.: Dissociation constants of carbonic acid in seawater as a function of salinity and temperature, *Mar. Chem.*, 100, 80–94, 2006.

Mosby, H. A.: The waters of the Atlantic Antarctic Ocean, *Scientific Results of the Norwegian Antarctic Expedition 1927–1928*, 11, 1–131, edited by: J. Dybwad, Oslo, 1934.

Orr, J. C., Fabry, V. J., Aumont, O., Bopp, L., Doney, S. C., Feely, R. A., Gnanadesikan, A., Gruber, N., Ishida, A., Joos, F., Key, R. M., Lindsay, K., Maier-Reimer, E., Matear, R., Monfray, P., Mouchet, A., Najjar, R. G., Plattner, G.-K., Rodgers, K. B., Sabine, C. L., Sarmiento, J. L., Schlitzer, R., Slater, R. D., Totterdell, I. J., Weirig, M.-F., Yamanaka, Y., and Yool, A.:

## An ocean acidification sensitivity study

A. Weeber et al.

Title Page

Abstract

Introduction

Conclusions

References

Tables

Figures



Back

Close

Full Screen / Esc

Printer-friendly Version

Interactive Discussion



Anthropogenic ocean acidification over the twenty-first century and its impact on calcifying organisms, *Nature*, 437, 681–686, 2005.

Pierrot, D., Neill, C., Sullivan, K., Castle, R., Wanninkhof, R., Lüger, H., Johannessen, T., Olsen, A., Feely, R. A., and Cosca, C. E.: Recommendations for autonomous underway  $p\text{CO}_2$  measuring systems and data reduction routines, *Deep-Sea Res. Pt. II*, 56, 512–522, 2009.

Raupach, M. R., Gloor, M., Sarmiento, J. L., Canadell, J. G., Frölicher, T. L., Gasser, T., Houghton, R. A., Le Quéré, C., and Trudinger, C. M.: The declining uptake rate of atmospheric  $\text{CO}_2$  by land and ocean sinks, *Biogeosciences*, 11, 3453–3475, doi:10.5194/bg-11-3453-2014, 2014.

Ries, J. B., Cohen, A. L., and McCorkle, D. C.: Marine calcifiers exhibit mixed responses to  $\text{CO}_2$ -induced ocean acidification, *Geology*, 37, 1131–1134, 2009.

Roden, N. P., Shadwick, E. H., Tilbrook, B., and Trull, T. W.: Annual cycle of carbonate chemistry and decadal change in coastal Prydz Bay, East Antarctica, *Mar. Chem.*, 155, 135–147, 2013.

Royal-Society.: Ocean acidification due to increasing atmospheric carbon dioxide, London: The Royal Society, 223 pp., 2005.

Sabine, C. L., Feely, R. A., Gruber, N., Key, R. M., Lee, K., Bullister, J., Wanninkhof, R., Wong, C. S., Wallace, D. W. R., Tilbrook, B., Millero, F. J., Peng, T.-H., Kozyr, A., Ono, T., and Rios, A. F.: The oceanic sink for anthropogenic  $\text{CO}_2$ , *Science*, 305, 367–371, 2004.

Sarmiento, J. L. and Gruber, N.: *Ocean Biogeochemical Dynamics*, Princeton University Press, Princeton, 2006.

Sedwick, P. N. and DiTullio, G. R.: Regulation of algal blooms in Antarctic shelf waters by the release of iron from melting sea ice, *Geophys. Res. Lett.*, 24, 2515–2518, 1997.

Seibel, B. A. and Dierssen, H. M.: Cascading trophic impacts of reduced biomass in the Ross Sea, Antarctica: Just the tip of the iceberg?, *Biol. Bull.*, 205, 93–97, 2003.

Shadwick, E. H., Trull, T. W., Thomas, H., and Gibson, J. A. E.: Vulnerability of Polar Oceans to Anthropogenic Acidification: Comparison of Arctic and Antarctic Seasonal Cycles, *Scientific reports*, 3, 2339, doi:10.1038/srep02339, 2013.

Smith, W. O. and Nelson, D. M.: Phytoplankton bloom produced by a receding ice edge in the Ross Sea: spatial coherence with the density field, *Science*, 227, 163–166, 1985.

Smith, W. O. and Nelson, D. M.: Importance of ice edge phytoplankton production in the Southern Ocean, *BioSciences*, 36, 251–257, 1986.

Solomon, S., Plattner, G. K., Knutti, R., and Friedlingstein, P.: Irreversible climate change due to carbon dioxide emissions, *P. Natl. Acad. Sci. USA*, 106, 1704–1709, 2009.

## An ocean acidification sensitivity study

A. Weeber et al.

Title Page

Abstract

Introduction

Conclusions

References

Tables

Figures



Back

Close

Full Screen / Esc

Printer-friendly Version

Interactive Discussion



Steinacher, M., Joos, F., Frölicher, T. L., Plattner, G.-K., and Doney, S. C.: Imminent ocean acidification in the Arctic projected with the NCAR global coupled carbon cycle-climate model, *Biogeosciences*, 6, 515–533, doi:10.5194/bg-6-515-2009, 2009.

Steinacher, M., Joos, F., Frölicher, T. L., Bopp, L., Cadule, P., Cocco, V., Doney, S. C., Gehlen, M., Lindsay, K., Moore, J. K., Schneider, B., and Segschneider, J.: Projected 21st century decrease in marine productivity: a multi-model analysis, *Biogeosciences*, 7, 979–1005, doi:10.5194/bg-7-979-2010, 2010.

Swart, S., Speich, S., Ansorge, I. J., and Lutjeharms, J. R. E.: An altimetry-based gravest empirical mode south of Africa: 1. Development and validation, *J. Geophys. Res.*, 115, C03002, doi:10.1029/2009JC005299, 2010.

Swart, S., Thomalla, S. J., Ansorge, I. J., and Monteiro, P. M. S.: Mesoscale features and phytoplankton biomass at the GoodHope transect in the Southern Ocean during austral summer, *Afr. J. Mar. Sci.*, 32, 511–524, doi:10.2989/1814232X.2012.749811, 2012.

Taylor, M. H., Losch, M., and Bracher, A.: On the drivers of phytoplankton blooms in the Antarctic marginal ice zone: A modeling approach, *J. Geophys. Res.-Oceans*, 118, 63–75, 2013.

Thomalla, S. J., Fauchereau, N., Swart, S., and Monteiro, P. M. S.: Regional scale characteristics of the seasonal cycle of chlorophyll in the Southern Ocean, *Biogeosciences*, 8, 2849–2866, doi:10.5194/bg-8-2849-2011, 2011.

Wanninkhof, R. and Thoning, K.: Measurement of fugacity of CO<sub>2</sub> in surface water using continuous and discrete sampling methods, *Mar. Chem.*, 44, 189–205, 1993.

Yamamoto, A., Kawamiya, M., Ishida, A., Yamanaka, Y., and Watanabe, S.: Impact of rapid sea-ice reduction in the Arctic Ocean on the rate of ocean acidification, *Biogeosciences*, 9, 2365–2375, doi:10.5194/bg-9-2365-2012, 2012.

Zeebe, R. E. and Wolf-Gladrow, D.: CO<sub>2</sub> in seawater: equilibrium, kinetics, isotopes, volume 65, Elsevier Science Ltd., 2001.

Zhang, H. M., Reynolds, R. W., and Bates, J. J.: Blended and gridded high resolution global sea surface wind speed and climatology from multiple satellites: 1987–present, *American Meteorological Society*, 2006, Annual Meeting, Paper P. Vol. 2, 2006.

## An ocean acidification sensitivity study

A. Weeber et al.

**Table 1.** Mean monthly aragonite saturation state ( $\Omega_A$ ) for the summers of 2009, 2010, 2010/2011 and 2012, showing the interannual variability and the change in  $\Omega_A$  ( $\Delta\Omega_A$ ) from an estimated winter minimum ( $\Omega_{AW}$ ) of 1.3 to the summer maximum ( $\Omega_{AS}$ ) during all years.

| Year      | Mean $\Omega_A$ |                 |                 | $\Omega_{AS}$ | $\Delta\Omega_A$<br>( $\Omega_{AW} - \Omega_{AS}$ ) |
|-----------|-----------------|-----------------|-----------------|---------------|---|
|           | Dec             | Jan             | Feb             |               |   |
| 2009      |                 | $1.97 \pm 0.16$ | $1.81 \pm 0.09$ | 2.32          | 1.02  |
| 2010      |                 | $1.51 \pm 0.06$ | $1.59 \pm 0.06$ | 1.76          | 0.46  |
| 2010/2011 | $1.61 \pm 0.17$ | $1.8 \pm 0.32$  | $1.99 \pm 0.18$ | 2.32          | 1.02  |
| 2012      |                 | $1.5 \pm 0.14$  | $1.54 \pm 0.13$ | 1.89          | 0.59  |

[Title Page](#)
[Abstract](#)
[Introduction](#)
[Conclusions](#)
[References](#)
[Tables](#)
[Figures](#)
[Back](#)
[Close](#)
[Full Screen / Esc](#)
[Printer-friendly Version](#)
[Interactive Discussion](#)


## An ocean acidification sensitivity study

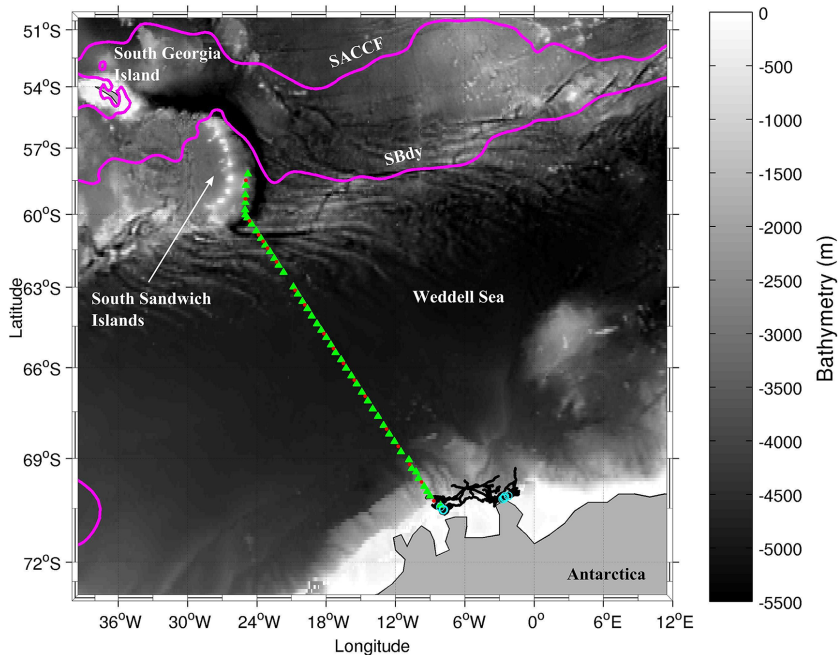
A. Weeber et al.

**Table 2.** Mean monthly aragonite saturation state ( $\Omega_A$ ) calculated when  $\text{CO}_2$  increased by  $160 \mu\text{atm}$  (predicted for the year 2050) and when  $\text{CO}_2$  concentration are doubled (predicted for the year 2100) for optimal and late summer sea ice thaw conditions.

| Timing of Sea Ice Thaw   | $\Omega_A$ predicted for 2050 |                    |                    | Summer mean        | $\Omega_A$ predicted for 2100 |                    |                    | Summer mean        |
|--------------------------|-------------------------------|--------------------|--------------------|--------------------|-------------------------------|--------------------|--------------------|--------------------|
|                          | Dec                           | Jan                | Feb                |                    | Dec                           | Jan                | Feb                |                    |
| Optimal (early December) | 01.14<br>$\pm 0.1$            | 1.28<br>$\pm 0.12$ | 1.32<br>$\pm 0.09$ | 1.25<br>$\pm 0.1$  | 0.9<br>$\pm 0.12$             | 1.08<br>$\pm 0.14$ | 1.13<br>$\pm 0.12$ | 1.04<br>$\pm 0.13$ |
| Late (early January)     |                               | 1.03<br>$\pm 0.03$ | 1.1<br>$\pm 0.06$  | 1.06<br>$\pm 0.05$ |                               | 0.78<br>$\pm 0.05$ | 0.86<br>$\pm 0.08$ | 0.82<br>$\pm 0.07$ |

[Title Page](#)
[Abstract](#)
[Introduction](#)
[Conclusions](#)
[References](#)
[Tables](#)
[Figures](#)

[Back](#)
[Close](#)
[Full Screen / Esc](#)
[Printer-friendly Version](#)
[Interactive Discussion](#)

**Figure 1.** Map showing stations for all years, underway sampling region (black dots), repeat ice shelf CTD stations (cyan circles) and the January 2011 CTD (red dots) UCTD (green triangles) stations. The mean locations of the southern ACC front (SACCF) and the southern boundary of the ACC (SBdy), as determined from satellite altimetry (Swart et al., 2010), are depicted with magenta lines. The regional bathymetry (ETOPO2) is overlaid (m below sea level).

An ocean acidification sensitivity study

A. Weeber et al.

Title Page

Abstract

Introduction

Conclusions

References

Tables

Figures

◀

▶

◀

▶

Back

Close

Full Screen / Esc

Printer-friendly Version

Interactive Discussion



## An ocean acidification sensitivity study

A. Weeber et al.

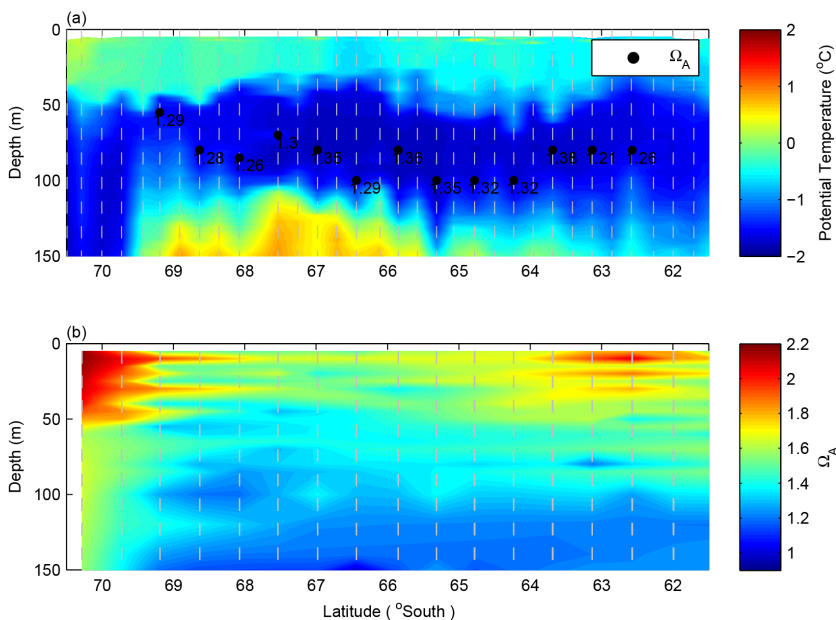


**Figure 2.** (a) Aragonite saturation state ( $\Omega_A$ ) at the depths where potential temperature is at a minimum, overlaid on the potential temperature section between South Gergia and the ice shelf, Antarctica. CTD stations are indicated with grey lines. (b) Aragonite saturation state ( $\Omega_A$ ) from bottle data, CTD stations where TA and DIC were sampled are indicated with grey lines.

Title Page

Abstract

Introduction

Conclusions

References

Tables

Figures

◀

▶

◀

▶

Back

Close

Full Screen / Esc

Printer-friendly Version

Interactive Discussion



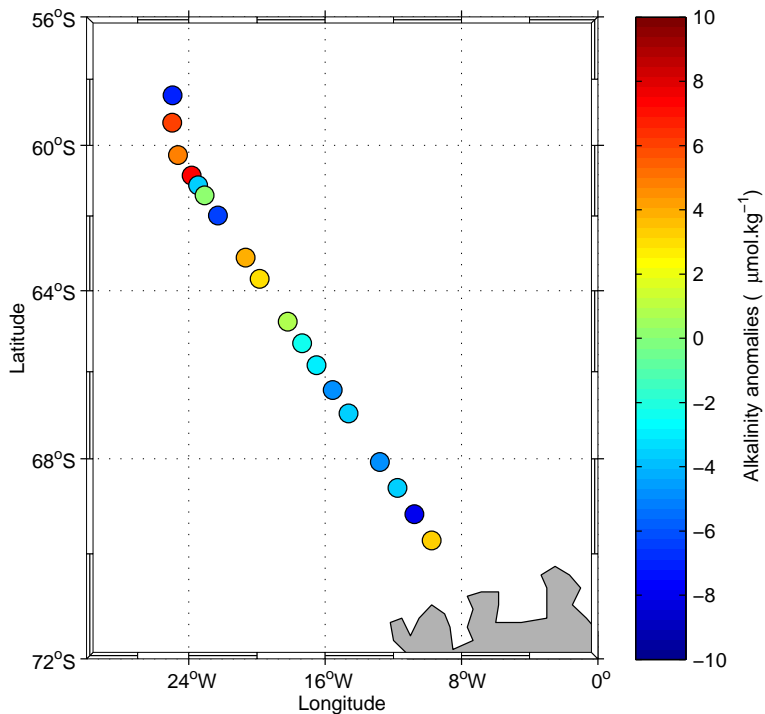


**Figure 3.** Alkalinity anomalies (calculated TA minus measured TA) between 1st to 20th January 2011, between 70–58° S 9–25° W. CTD stations were conducted on the way back from South Georgia Island to the Antarctic ice shelf. In the study region (71–68° S) these anomalies were on average  $-3 \mu\text{mol kg}^{-1}$ .

An ocean acidification sensitivity study

A. Weeber et al.

Title Page

Abstract

Introduction

Conclusions

References

Tables

Figures



Back

Close

Full Screen / Esc

Printer-friendly Version

Interactive Discussion



## An ocean acidification sensitivity study

A. Weeber et al.

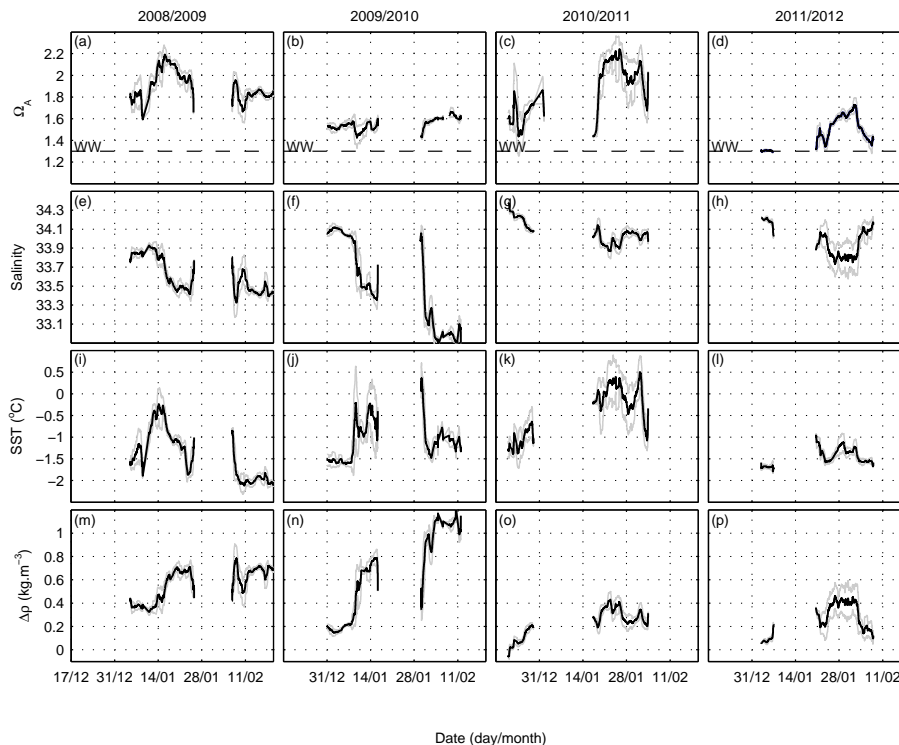


**Figure 4.** (a–d) Aragonite saturation state ( $\Omega_A$ ), (e–h) salinity, (i–l) sea surface temperature (SST) and (m–p) change in density from Winter Water (WW), ( $\rho \sim 1027.61 \text{ kg m}^{-3}$ ) to summer surface water ( $\Delta\rho$ ), for four consecutive summer periods that range from 17 December to 18 February. The daily mean is shown by the black line with  $\pm$ one standard deviation shown by the grey lines. The dashed line (a–d) shows the mean WW  $\Omega_A$ .

Title Page

Abstract

Introduction

Conclusions

References

Tables

Figures

◀

▶

◀

▶

Back

Close

Full Screen / Esc

Printer-friendly Version

Interactive Discussion



## An ocean acidification sensitivity study

A. Weeber et al.

Title Page

Abstract

Introduction

Conclusions

References

Tables

Figures



Back

Close

Full Screen / Esc

Printer-friendly Version

Interactive Discussion

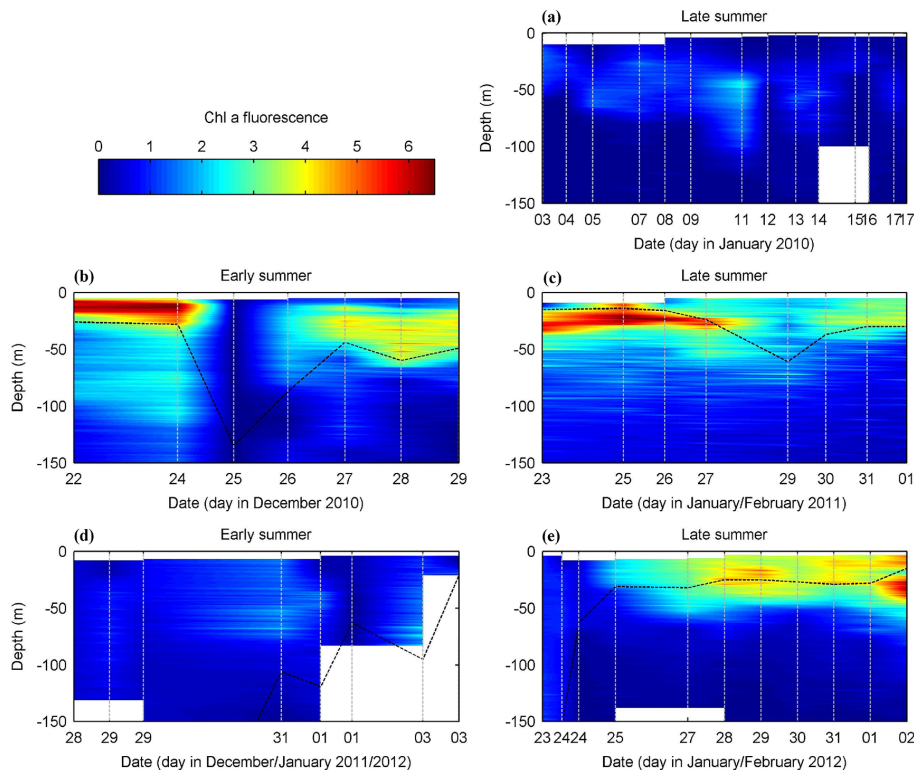


**Figure 5.** Chlorophyll *a* profiles during early and late summer periods in (a) 2010, (b) 2010, (c) 2011, (d) 2011/2012 and (e) 2012. CTDs were deployed at the ice shelf in all years between 2–9° W and 70–71° S (dashed gray lines) and the mixed layer depth was calculated from density ( $\Delta\rho = 0.03 \text{ kg m}^{-3}$  referenced from 10 m depth, dashed black line).

## An ocean acidification sensitivity study

A. Weeber et al.

Title Page

Abstract

Introduction

Conclusions

References

Tables

Figures

◀

▶

◀

▶

Back

Close

Full Screen / Esc

Printer-friendly Version

Interactive Discussion

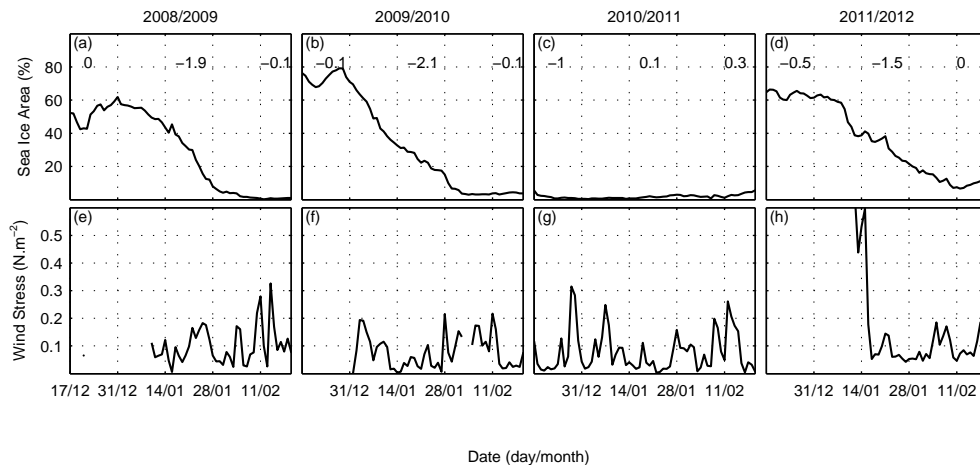


**Figure 6.** (a–d) Mean daily % of sea ice cover and (e–h) mean daily wind stress ( $\text{N m}^{-2}$ ) for four consecutive summer periods between 17 December to 18 February for the region  $68\text{--}71^\circ\text{S}$ ;  $0\text{--}10^\circ\text{W}$ .



## An ocean acidification sensitivity study

A. Weeber et al.

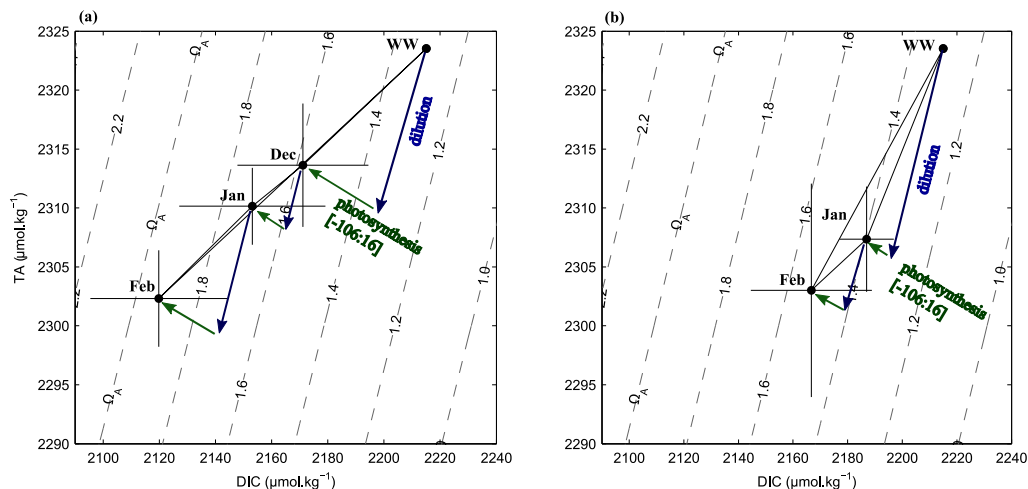


**Figure 8.** Vector plots (DIC-TA) showing the seasonal evolution of mean December, January and February total alkalinity (TA) and dissolved inorganic carbon (DIC) at the ice shelf. Winter Water (WW) conditions calculated from CTDs ( $\Omega_A$  WW  $\sim$  1.3). Vectors depict the rate of dilution and photosynthesis that altered TA and DIC, contours show aragonite saturation state ( $\Omega_A$ ) with temperature =  $-1^\circ\text{C}$  salinity = 33.3. The two seasonal extremes are depicted: **(a)** a high  $\Omega_A$  summer during December 2010, January and February 2011, **(b)** a low  $\Omega_A$  summer during January and February 2012. Total seasonal dilution is comparable so the difference in  $\Omega_A$  in due primarily to photosynthesis.

Title Page

Abstract

Introduction

Conclusions

References

Tables

Figures



Back

Close

Full Screen / Esc

Printer-friendly Version

Interactive Discussion

